7344 J. Med. Chem. 2010, 53, 7344–7355
DOI: 10.1021/jm100925m

Journal of Medicinal Chemistry Article

Design, Synthesis, Radiolabeling, and in Vivo Evaluation of Carbon-11 Labeled *N*-[2-[4-(3-Cyanopyridin-2-yl)piperazin-1-yl]ethyl]-3-methoxybenzamide, a Potential Positron Emission Tomography Tracer for the Dopamine D_4 Receptors

Enza Lacivita,[†] Paola De Giorgio,[†] Irene T. Lee,[‡] Sean I. Rodeheaver,[‡] Bryan A. Weiss,[‡] Claudia Fracasso,[§] Silvio Caccia,[§] Francesco Berardi,[†] Roberto Perrone,[†] Ming-Rong Zhang,[∥] Jun Maeda,[∥] Makoto Higuchi,[∥] Tetsuya Suhara,[∥] John A. Schetz,[‡,⊥,#,∞,×] and Marcello Leopoldo*[,†,×]

[†]*Dipartimento Farmaco-Chimico, Università degli Studi di Bari "A. Moro", Via Orabona, 4, 70125, Bari, Italy,* [‡]*Department of Pharmacology and Neuroscience, University of North Texas Health Science Center, 3500 Camp Bowie Boulevard, Fort Worth, Texas 76107-2699, United States,* [§]*Istituto di Ricerche Farmacologiche "Mario Negri", Via La Masa 19, 20156 Milan, Italy,* [∥]*Molecular Imaging Center, National Institute of Radiological Sciences, 9-1, 4-Chome, Anagawa, Inage-ku, 263-8555, Chiba, Japan,* [⊥]*Department of Psychiatry, Texas College of Osteopathic Medicine, Fort Worth, Texas 76107, United States,* [#]*Department of Health Management and Policy, School of Public Health, Fort Worth, Texas 76107, United States, and* [∞]*Department of Biology, University of Texas at Arlington, Arlington, Texas 76109, United States.*
[×] *J.A.S. and M.L. contributed equally to this study.*

Received July 22, 2010

Here we describe the design, synthesis, and evaluation of physicochemical and pharmacological properties of D_4 dopamine receptor ligands related to *N*-[2-[4-(4-chlorophenyl)piperazin-1-yl]ethyl]-3-methoxybenzamide (**2**). Structural features were incorporated to increase affinity for the target receptor, to improve selectivity over D_2 and σ_1 receptors, to enable labeling with carbon-11 or fluorine-18, and to adjust lipophilicity within the range considered optimal for brain penetration and low nonspecific binding. Compounds **7** and **13** showed the overall best characteristics: nanomolar affinity for the D_4 receptor, >100-fold selectivity over D_2 and D_3 dopamine receptors, 5-HT_{1A}, 5-HT_{2A}, and 5-HT_{2C} serotonin receptors and σ_1 receptors, and log P = 2.37−2.55. Following intraperitoneal administration in mice, both compounds rapidly entered the central nervous system. The methoxy of *N*-[2-[4-(3-cyanopyridin-2-yl)piperazin-1-yl]ethyl]-3-methoxybenzamide (**7**) was radiolabeled with carbon-11 and subjected to PET analysis in non-human primate. [^{11}C]**7** time-dependently accumulated to saturation in the posterior eye in the region of the retina, a tissue containing a high density of D_4 receptors.

Introduction

The dopamine D_4 receptor belongs to the D_2-like receptor family which is characterized by its ability to interact with $G_{i/o}$ proteins resulting in inhibition of adenylyl cyclase. Early interest in the D_4 receptor originated from the finding that the D_2-like receptor antagonist clozapine, an atypical antipsychotic drug with high antipsychotic efficacy and reduced extrapyramidal and neuroendocrine side effects, had 10 times higher affinity for this receptor than for other D_2-like receptor subtypes.[1,2] This resulted in an intense search for dopamine D_4 antagonists.[3] However, L-745,870 (Chart 1), one of the first highly D_4-selective antagonists to be reported, failed to show antipsychotic potential in animal models.[4] In placebo-controlled clinical trials, the more bioavailable congener of **1** (L-745,870) named L-750,667 (Chart 1) did not alleviate any of the symptoms of schizophrenia.[5] Instead, there was a trend toward a worsening of psychotic symptoms. Although these findings seemed to exclude the D_4 receptor as an antipsychotic drug target, later in vitro studies with **1** provided evidence for its weak partial agonist activity.[6,7] Subsequently, the selective D_4 ligand FAUC 213 (Chart 1), structurally related to **1**, was characterized as a "neutral antagonist" using a different measure of functional activity (thymidine incorporation instead of cAMP accumulation).[8] Years later, a dose of this same ligand, which reduced amphetamine-induced increased locomotor activity, was demonstrated to have atypical antipsychotic potential in animal models predictive of antipsychotic efficacy in humans.[9] This is in contrast to the structurally distinct D_4-selective neutral antagonist PNU-101,387G (sonepiprazole) (Chart 1), which has no demonstrable antipsychotic activity in humans.[10]

The D_4 receptor has been suggested as a candidate gene for novelty seeking behavior[11−14] and attention deficit hyperactivity disorder (ADHD[a]),[15−18] although the latter association or its basis has been questioned.[19−21] While certain antagonists of the D_4 receptor reduced hyperactivity in a neonatal 6-hydroxydopamine lesioned rat model of ADHD,[22] the hyperactivity due to neonatal lesioning appears to be mediated by compensatory changes in serotonin transporters.[23] More recently, the D_4 agonist A-412997 (Chart 1) was shown to improve cognitive function in both a five-trial inhibitory avoidance paradigm and the social recognition model, which are two animal models thought to be predictive of anti-ADHD efficacy.[24]

The D_4 receptor has been implicated in the control of penile tumescence. For instance, D_4 selective agonists like ABT-724

*To whom correspondence should be addressed. Phone: +39 080 5442798. Fax: +39 080 5442231. E-mail: leopoldo@farmchim.uniba.it.

[a] Abbreviations: ADHD, attention deficit hyperactivity disorder; PET, positron emission tomography; GPCR, G-protein-coupled receptor; BBB, blood−brain barrier.

 Published on Web 09/27/2010

Chart 1. Representative Selective Dopamine D_4 Receptor Ligands

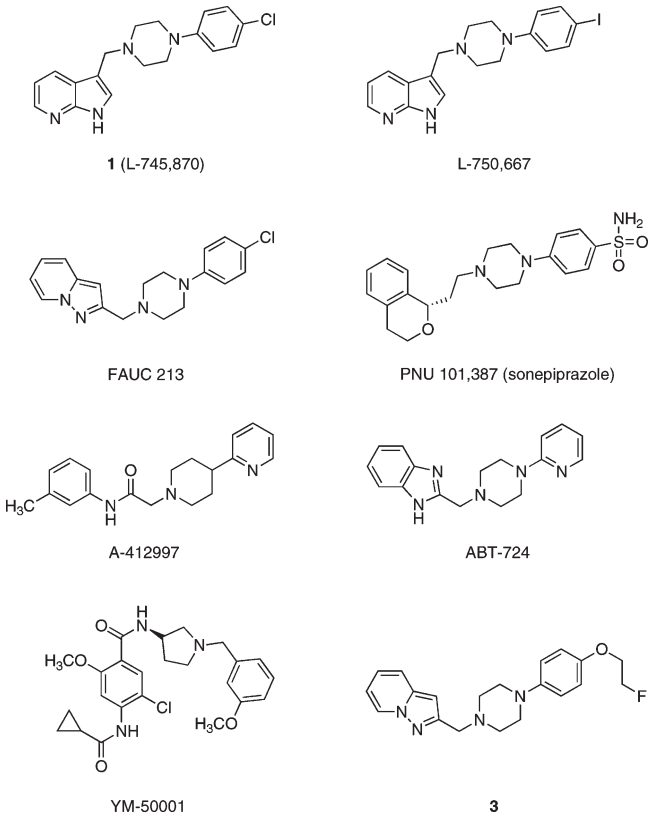

(Chart 1) produce erectogenesis in animal models without nausea.[25] However, studies in rats support a role for the D_3 receptor, but not the D_4 receptor, in the induction of penile erection by D_2-like agonists in rodents.[26] Although the D_4 receptor is expressed at low levels in the brain, much higher densities of this receptor are expressed in the retina.[27] Dopamine, via D_4 receptors, normally modulates the cascade that couples light responses to adenylyl cyclase activity in photoreceptor cells in the retina.[28,29]

To better understand dopamine D_4 receptor biology in vivo, a suitable D_4 receptor positron emission tomography (PET) tracer would be a powerful tool allowing noninvasive D_4 receptor imaging. A number of attempts have been made to identify a D_4-selective PET radioligand.[30−36] In 2000, Langer and co-workers reported an attempt to visualize the dopamine D_4 receptor in primate brain with [^{11}C]PB-12 (compound **2**, Table 1).[32] The radioligand was of little use in visualizing D_4 receptors because it exhibited a very high background due to nonspecific binding. Similar results were obtained 2 years later by Zhang and co-workers who prepared and tested [^{11}C]**2** and [^{11}C]YM-50001 (Chart 1) with both radioligands being unsuitable for D_4 receptor imaging with PET.[34] In each case, it was suggested that the high nonspecific binding of [^{11}C]**2** could be due to its relatively high lipophilicity (ClogP = 3.72).[37] More recently, Prante and co-workers reported on the rational design of a series of pyrazolo[1,5-*a*]-pyridine-based dopamine D_4 receptor ligands for potential use as PET ligands. However, the most promising radioligand of the series, [^{18}F]**3** (ClogP = 2.9) (Chart 1), was only tested in rat brain slices by in vitro autoradiography.[36] Thus, to date, there are no verified examples of a D_4-selective PET tracer.

An adequate PET tracer for neuroreceptor visualization must fulfill many criteria:[38,39] high affinity for the target receptor (usually in the nanomolar range); selectivity for its target (>100-fold); ease of labeling with ^{11}C or ^{18}F at high specific radioactivity; safe administration at low tracer dose; high blood−brain barrier (BBB) penetrance; inability to serve as a substrate for efflux transporters; low nonspecific binding; suitable brain pharmacokinetics in relation to radiolabel half-life (observable brain uptake and washout kinetics); lack of troublesome radiometabolites. Of particular importance with respect to BBB penetration and low nonspecific binding is tracer lipophilicity. In general, brain penetration by passive diffusion of molecules across the BBB becomes poor when the log *P* is greater than 4.0, molecular weight is larger than 450 Da, and the number of hydrogen bond donors is greater than 5. However, if molecules are too hydrophilic, their BBB passage is prevented as well. It has been reported for many drug classes that the optimum log *P* value for central nervous system (CNS) targeted drugs lies between 2.0 and 3.5. Moreover, high lipophilicity attributed to adhesion to proteins and lipids tends to increase nonspecific binding, an essentially nonsaturable component of the total tissue uptake of a radioligand. Therefore, it appears that there is an optimal range of lipophilicity for brain radioligands, wherein brain uptake is high and nonspecific binding comparatively weak. From data in the literature, log *P* = 3.5 appears to be the acceptable upper limit of lipophilicity for a PET radioligand.[40]

Here we describe the synthesis and in vitro characterization of an improved series of D_4 receptor agents derived from our lead compound **2**,[41−43] which we rationally designed specifically for use as a PET radiotracer. By use of our newly developed selection criteria and assay cascade, one of a dozen compounds was selected for radiolabeling with carbon-11 and PET studies in monkey brain.

Chemistry

The synthesis of the final compounds is depicted in Scheme 1. The preparation of the target compounds required the key amines **18a**−**f**. Among these, 4-(4-chlorophenyl)-1-piperazineethanamine (**18a**) and 4-(4-methylphenyl)-1-piperazineethanamine (**18b**) were prepared according to the literature.[44] Amines **18c**−**e** were prepared as follows: the appropriate 1-arylpiperazine was alkylated with 2-haloethanol to the corresponding alcohol **15c**−**e**. These latter were subsequently condensed, under Mitsunobu conditions, with phthalimide to give **16c**−**e**, which were hydrolyzed with hydrazine hydrate to afford primary amines **18c**−**e**. An alternative synthetic route was followed to prepare amine **18f**: 1-(5-chloro-2-pyridinyl)-piperazine[45] was first alkylated with chloroacetonitrile and then treated with borane dimethyl sulfide complex to afford the desired amine **18f**. The final compounds were prepared by condensing 3-methoxy- or 4-fluorobenzoic acid with amines **18a**−**f** in the presence of 1,1′-carbonyldiimidazole.

Results and Discussion

Lipophilicity Evaluation. The pivotal role of PET tracer lipophilicity is well recognized, and it has been reviewed in depth by Waterhouse.[40] Lipophilicity can be evaluated in various theoretical and experimental ways. The most common experimental lipophilicity measurement involves partitioning of a compound between octanol and aqueous solution (log *P*). The log *P* refers to partitioning of the neutral molecule species and log $D_{7.4}$ the partitioning of all species present in solution at a given pH, which accounts for solubility effects associated with ionization. When lipophilicity is expressed as log *P* or log $D_{7.4}$, compounds that seem most effective for

Table 1. Lipophilicity Values and Binding Affinities at Dopamine D_4 Receptors of the Target Benzamides

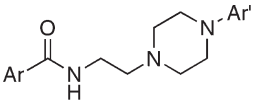

cpd	Ar	Ar'	ClogP	logP	$logD_{7.4}$	pKa	D_4 K_i, nM ± SEM
2		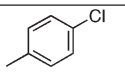	3.72	3.31	3.28	6.19 ± 0.08	4.97 ± 1.00
4		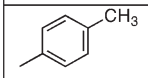	3.33	2.83	2.78	6.46 ± 0.01	9.21 ± 0.83
5		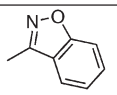	2.71	3.08	3.05	6.24 ± 0.02	1.93 ± 0.38
6		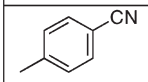	2.66	3.08	3.03	6.41 ± 0.05	63.95 ± 6.04
7		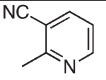	1.50	2.55	2.47	6.71 ± 0.03	1.52 ± 0.20
8		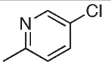	2.67	3.29	3.24	6.45 ± 0.04	11.29 ± 0.90
9	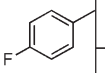	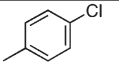	3.86	3.75	3.70	6.46 ± 0.01	1.76 ± 0.58
10		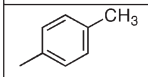	3.33	2.98	2.95	6.31 ± 0.03	2.64 ± 0.47
11		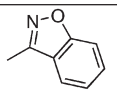	2.86	3.79	3.75	6.43 ± 0.05	0.34 ± 0.15
12		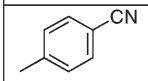	2.81	3.07	3.02	6.43 ± 0.06	32.71 ± 5.21
13		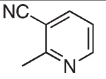	1.64	2.37	2.33	6.40 ± 0.01	0.93 ± 0.18
14		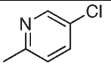	2.82	3.42	3.36	6.58 ± 0.03	2.92 ± 0.68

imaging have log *P* or log $D_{7.4}$ of < 3.5. On such a basis, we have modified our reference compound **2** and designed compounds **4**−**14** which showed computer estimated values of lipophilicity below the guideline value (3.5). Then, the experimental log *P*, log $D_{7.4}$, and pK_a values of **4**−**14** were determined by potentiometric titrations (Table 1). Considering the pK_a values of target compounds, it can be deduced that the percentage of protonated species at physiological pH is not very high, and this accounts for the similarities between log *P* and log $D_{7.4}$ values. Experimental log *P* values were, however, different from the calculated values. The largest difference (1.05 log units) was shown in the case of compound **7** (ClogP = 1.50 vs log *P* = 2.55), whereas the smallest (0.26 log units) was for **12** (ClogP = 2.81 vs log *P* = 2.37). While the explanation of such differences is beyond the scope of this study, these data confirm that the lipophilicity of a molecule is the result of all intermolecular solute−solvent interactions in both aqueous and organic solvents and not only the sum of the contribution of isolated fragments. In fact, the difference between log *P* values and ClogP can, and in our case does, vary among structurally related compounds. For example, compounds **5** and **11** have a difference between the calculated and experimental log *P* of 0.37 and 0.93, respectively; for **7** and **13**, the difference was 1.05 and 0.43, respectively. In spite of these discrepancies, all the experimental log *P* values were below the guideline value with the exception of those for **9** and **11**, which had log *P* values of 3.75 and 3.79, respectively. Therefore, in those cases when lipophilicity must fall within a narrow range and ClogP values are borderline, an experimental determination is prudent.

Rational Design and Structure−Affinity Relationships. All the target compounds were designed taking into account the structural requirements for an adequate PET tracer as detailed in the Introduction. Compounds **4**−**8** have a methoxy group

Scheme 1[a]

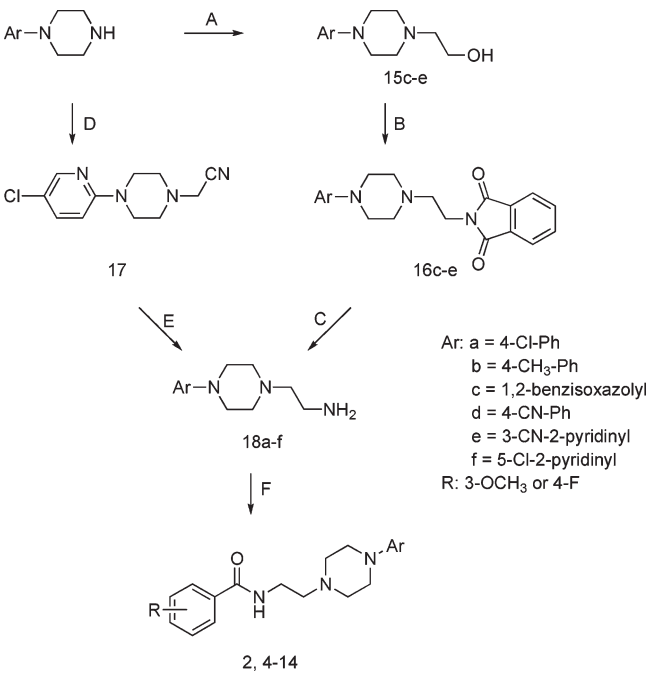

[a] Reagents: (A) 2-chloroethanol or 2-bromoethanol, K_2CO_3; (B) phthalimide, Ph_3P, DEAD; (C) (i) hydrazine hydrate, (ii) conc HCl; (D) chloroacetonitrile, K_2CO_3; (E) borane−methyl sufide complex; (F) 3-methoxy- or 4-fluorobenzoic acid, CDI.

that can be easily accessed in the [^{11}C] radiolabeled form via the corresponding phenol derivative. Compounds **9**−**14** possess the 4-fluorobenzamide group which can be obtained in the [^{18}F] radiolabeled form via the corresponding 4-nitrobenzamide or 4-tributyltinphenyl analogue. The structural modifications of **2** were also guided by the previous structure−affinity relationship studies. Thus, in the first group of compounds the *N*-[2-(4-arylpiperazin-1-yl)ethyl]-3-methoxybenzamide structure was left unchanged (compounds **4**−**8**, Table 1). The modification was limited to the aryl group linked to the piperazine ring. In particular, replacement of −Cl in **2** with $-CH_3$ led to **4** which has only 2-fold lower affinity for the D_4 receptor than **2**. On the other hand, replacement of −Cl in **2** with −CN gave **6** which had considerably less affinity than **2** (K_i = 63.95 nM). Replacement of the phenyl ring in **2** with a 2-pyridyl gave **8** which demonstrated only 2-fold less affinity than **2**. In a previous study we found that *N*-[4-[4-(1,2-benzisoxazol-3-yl)piperazin-1-yl]butyl]-3-methoxybenzamide displayed high affinity (K_i = 7.58 nM) for the D_4 receptor.[46] Thus, we wanted to evaluate if a shorter alkyl chain (ethyl vs butyl) increased affinity for the D_4 receptor. Compound **5** displayed higher affinity (K_i = 1.93 nM) than either the butyl homologue cited above and **2**. The replacement of 4-chlorophenyl group in **2** by the 3-cyano-2-pyridinyl one (**7**) was undertaken because a number of D_4 ligands reported in the literature were characterized by such a group.[47] This replacement was particularly beneficial because **7** had improved affinity for the D_4 receptor (K_i = 1.52 nM). A second set of derivatives were designed by replacing the 3-methoxybenzamide of **2**, **4**−**8** with a 4-fluorobenzamide (compounds **9**−**14**, Table 1). The 4-fluorobenzamides **9**−**14** possessed higher D_4 affinities than their 3-methoxy counterparts. The most notable increase in affinity was observed in the case of 1,2-benzisoxazol-3-yl derivative **11** which has approximately 6-fold higher affinity than the 3-methoxy analogue **5**. Also, the rank order of binding affinity among the derivatives was practically unchanged with the sole exception of 3-cyano-2-pyridinyl **13**, which had slightly less affinity than the 1,2-benzisoxazol-3-yl **11**. All in all, the proposed structural modifications led to a range of D_4 ligands possessing affinities higher than the lead compound **2**. Among them, **11** and **13** demonstrated subnanomolar K_i values. Subsequently, all compounds were evaluated at 1 μM for their ability to displace [^{3}H]methylspiperone from the rat cloned D_{2L} dopamine receptor (Table 2). Strong displacement was observed for compounds **5** and **11**, indicating that they have significant affinity for the D_{2L} receptor. Moderate displacement (40−50%) was observed for **9**, **10**, **13**, and **14**, whereas **2**, **4**, **6**−**8**, and **12**, had practically no effect on the specific binding of the radioligand to the D_{2L} receptor. Because some compounds touted as being D_4-selective actually have high affinity for the σ_1 receptor,[48] all compounds were evaluated at 1 μM for their ability to displace specifically bound [^{3}H]-(+)-pentazocine from the human cloned σ_1 receptor (Table 2). Little or no displacement (< 40%) was observed for all the tested compounds, indicating that they have little or no affinity for the σ_1 receptor. Taken together, these data indicate that compounds **7** and **13** have high selectivity for the D_4 receptor over D_{2L} and σ_1 receptors. Therefore, both compounds were evaluated further for potential interactions with selected other G-protein-coupled receptors (GPCRs) and for their functional properties at the D_4 receptor. While **7** and **13** had a similar binding profile for D_3, CB_1, and 5-HT_{2C} receptors, **7** had significantly less radioligand displacing activity at 5-HT_{1A} and 5-HT_{2A} receptors than **13** (Table 3). Both **7** and **13** were able to stimulate D_4 receptors measured as a decrease in forskolin-stimulated levels of cAMP accumulation (Figure 1), indicating that they have agonist properties.

Table 2. Displacement of Specifically Bound Radioligand from Cloned Dopamine D_{2L} and σ_1 Receptors by a Single High Concentration of Compound (1 μM)[a]

	% displacement ± SEM	
compd	D_{2L}	σ_1
2	7.8 ± 4.2	22 ± 7.2
4	7.6 ± 3.7	7.2 ± 8.4
5	84 ± 3.0	13 ± 4.2
6	0 ± 2.8	27 ± 15
7	4.4 ± 1.3	8.3 ± 6.2
8	5.8 ± 0.95	15 ± 8.4
9	48 ± 10	29 ± 3.2
10	29 ± 4.6	21 ± 4.6
11	89 ± 5.2	21 ± 2.9
12	0 ± 0.58	4.6 ± 2.1
13	32 ± 8.4	1.0 ± 3.7
14	43 ± 2.1	33 ± 1.9

[a] Nonspecific binding is defined by the following: 5 μM (+)-butaclamol displaced 100% of [^{3}H]MSP from D_{2L} receptors, and 5 μM BD1063 displaced 100% of [^{3}H]-(+)-pentazocine from σ_1 receptors.

Considering that a PET tracer needs to have high affinity for the target receptor and, in particular, it is preferable that the B_{max} clearly exceeds the K_d of the ligand (ideally $B_{max}/K_d > 10$),[49] one could ask if compounds **7** and **13** meet this requirement. D_4 receptor binding sites have previously been determined indirectly by the use of [^{3}H]NGD-94-1,[50] [^{3}H]PNU-101958,[51] and [^{3}H]nemonapride.[52] However, these studies have delivered controversial data on the distribution and concentration of D_4 receptor in the human and rat brain. For example, using [^{3}H]nemonapride in combination with **1**, raclopride, sulpiride,

Table 3. Displacement of Specifically Bound Radioligand by **7** and **13** from Cloned Human Dopamine D_3 Receptor, Cloned Serotonin Receptor Subtypes, and the CB_1 Cannabinoid Receptor by a Single High Concentration of Compound (1 μM)[a]

	% displacement ± SEM	
receptor	**7**	**13**
D_3	5.1 ± 1.1	7.2 ± 3.2
5-HT_{1A}	9.3 ± 5.9	29 ± 4.7
5-HT_{2A}	24 ± 4.7	53 ± 12
5-HT_{2C}	3.2 ± 3.8	0 ± 4.1
CB_1	6.5 ± 16	9.9 ± 0.1

[a] Nonspecific binding is defined by the following: 5 μM 7-OH-DPAT displaced 100% of [^{3}H]MSP from D_3 receptors; 5 μM NAN-190 displaced 100% of [^{3}H]-MPPF from 5-HT_{1A} receptors; 5 μM mianserin displaced 100% of [^{3}H]MSP from 5-HT_{2A} receptors; 5 μM mianserin displaced 100% of [^{3}H]mesulergine from 5-HT_{2C} receptors; 10 μM O-2050 displaced 100% of [^{3}H]CP55,940 from rat brain CB_1 receptors.

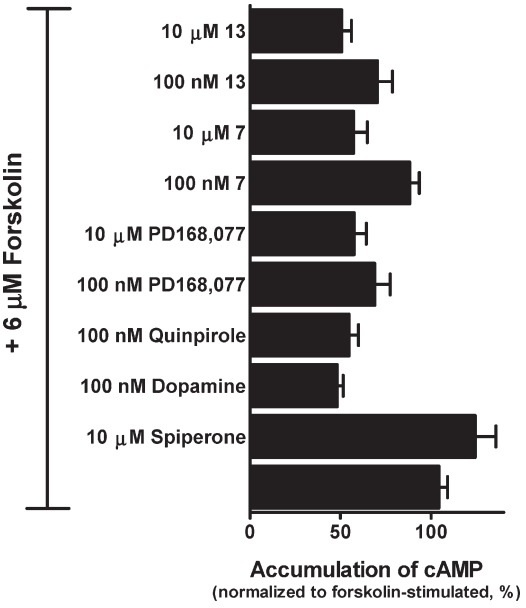

Figure 1. Compounds **7** and **13** are agonists of the cloned D_4 dopamine receptor as determined by $G_{i/o}$-mediated changes in intracellular cAMP. The D_4-selective antagonist spiperone, the D_4-selective agonist PD168,077, the D_2-like agonist (−)-quinpirole, and dopamine are shown for comparison.

and a σ receptor antagonist, a low density of D_4 receptors was observed (B_{max} = 8.9 fmol·(mg of protein)$^{-1}$) only in the hippocampus.[52] In contrast, Primus and co-workers used [^{3}H]NGD-94-1 and reported B_{max} values ranging from 8.9 to 28.9 fmol·(mg of protein)$^{-1}$ in hippocampal, cortical, and limbic regions.[50] Importantly, these values originate from homogenized tissue and do not necessarily reflect the tissue heterogeneity to be encountered in the intact brain in vivo.[53] Therefore, the concentration of D_4 receptor sites determined by indirect methods should be viewed with some caution, making the lack of precise B_{max} values for the D_4 receptor in the brain difficult to estimate the affinity value to be targeted when developing a D_4 PET tracer. Since compounds **7** and **13** had the best combination of lipophilicity, high affinity (K_i in the low nanomolar range), and selectivity for the D_4 receptor of the ligands listed in Table 1, they were selected for further testing in order to assess their potential of use in vivo as PET tracers.

Table 4. Mean ± SD (n = 3) Maximum Plasma and Brain Concentrations after ip Dosing of 10 mg/kg of Compounds **7** (after 30 min) and **13** (after 15 min) in Mice[a]

	concentration	
compd	plasma (μg/mL)	brain (μg/g)
7	0.37 ± 0.21 (0.22 ± 0.12)	0.14 ± 0.02 (< 0.1)
13	0.13 ± 0.10 (< 0.1)	0.47 ± 0.20 (< 0.1)

[a] Shown in parentheses is the N-dealkylated metabolite 1-(6-cyano-2-pyridyl)piperazine.

Disposition Studies in Mice with Compounds 7 and 13. Mice were given an intraperitoneal dose of the 4-fluorobenzamide **13** and the 3-methoxybenzamide **7** and were sacrificed at various times thereafter to obtain basic information on the concentrations of unchanged compound achieved in brain and their relationship with plasma concentrations. The presence of 1-(6-cyano-2-pyridyl)piperazine was also monitored in parallel because many N-substituted 1-arylpiperazines are reported to undergo metabolic N-dealkylation.[54] As shown in Table 4, compound **13** rapidly reached the systemic circulation with maximal plasma concentrations (C_{max}) 15 min after dosing (i.e., the first sampling time). However, these plasma concentrations were low and variable (0.13 ± 0.10 μg/mL) and rapidly fell below the limit of quantitation after 30 min (i.e., less than 0.1 μg/mL, using 0.2 mL of mouse plasma). Compound **7** peaked slightly later, yielding a higher mean C_{max} (0.37 ± 0.21 μg/mL at 30 min), and these concentrations were consistently detected only up to 60 min after dosing. Thus, in both cases the data did not permit adequate determination of a terminal elimination phase and the calculation of conventional pharmacokinetic parameters. This behavior may be partly due to a large presystemic biotransformation after intraperitoneal dosing because 1-arylpiperazine derivatives are generally extensively biotransformed before reaching the systemic circulation, and their clearance is almost entirely due to hepatic metabolism.[54] Concentrations of 1-(6-cyano-2-pyridyl)piperazine, however, were low for **7** (0.10−0.2 μg/mL) or not detectable for **13** (< 0.1 μg/mL) within 30−60 min of intraperitoneal dosing (10 mg/kg). This suggests that N-dealkylation of the aliphatic side chain may have contributed to but did not account for the first-pass effect and clearance of **7** and **13** in mice. Brain uptake was rapid for both derivatives: quantifiable levels were consistently evident up to 30 min for **7** and 60 min in the case of **13**. Mean brain C_{max} averaged 0.47 ± 0.20 μg/g for the 4-fluorobenzamide **13** (at 15 min post dose) and 0.14 ± 0.02 μg/g for the 3-methoxybenzamide **7** (at 30 min post dose), giving rise, at these times, to a mean brain-to-plasma concentration ratio higher for the more lipophilic fluorobenzamide derivative. While an accurate determination of whole brain exposure and brain-to-plasma distribution ratios was not possible, rough estimates based on the limits of quantification further suggested that the fluorobenzamide is concentrated in brain tissue of mice more than its methoxybenzamide analogue. In both cases the brain concentrations of the dealkylated metabolite 1-(6-cyano-2-pyridyl)piperazine were below the limit of detection within 180 min of dosing (about 0.1 μg/g, using approximately 200 mg of brain tissue).

These data indicated that both **7** and **13** can reach the brain and have fast uptake kinetics ideal for a PET tracer. Because of the relative ease of radiolabeling, compound **7** was selected as a PET D_4 tracer candidate.

Radiosynthesis of [^{11}C]7. Derivative **19**, the desmethyl precursor for ^{11}C-radiolabeling, was prepared as shown in

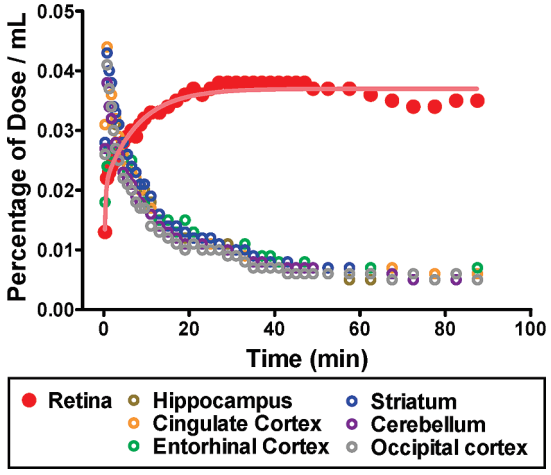

Figure 2. Time−activity curves of [^{11}C]**7** in seven CNS regions for 90 min in rhesus monkey.

Scheme 2[a]

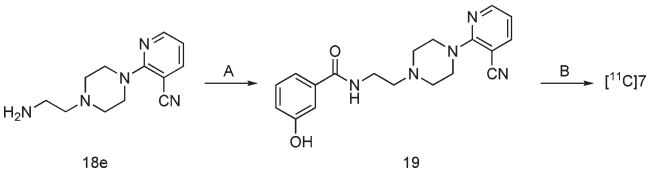

[a] Reagents: (A) 3-hydroxybenzoic acid, CDI; (B) [^{11}C]CH_3I, NaOH.

Scheme 2. 3-Hydroxybenzoic acid was condensed with 4-(3-cyanopyridin-2-yl)-1-piperazinoethanamine (**18e**) to give benzamide **19** in 40% yield. For the radiolabeling **19** was reacted with [^{11}C]CH_3I in DMF and 0.5 N NaOH to afford [^{11}C]**7** in an incorporation yield of 40.5 ± 10.8% (n = 4, determined by HPLC). Purification by semipreparative reverse-phase HPLC afforded [^{11}C]**7** (>99%). No significant peak of unreacted **19** was seen on the HPLC chromatogram of the final radioactive product. The retention time of [^{11}C]**7** on the analytical reverse-phase HPLC system was 6.2 min. The total synthesis time was about 28 min from the end of bombardment. The specific radioactivity at time of injection of [^{11}C]**7** was 2885 GBq/μmol, corresponding to a total injected dose of 150.3 MBq (52 pmol, 18 ng) in the monkey experiments.

PET Studies in Rhesus Monkey. After intravenous injection of [^{11}C]**7** in a male rhesus monkey, the uptake of [^{11}C]**7** in all brain regions peaked at 45 s and then the radioactivity rapidly declined, suggestive of no specific binding in these regions (Figure 2). About 3.1% of the injected radioactivity reached the brain at peak time. In contrast, radioactivity was markedly higher in the retina compared to the brain regions examined (Figure 3). The ratio of retinal radioactivity to the cerebral radioactivity was more than 6-fold at the end of the scanning period.

While [^{11}C]**7** did not accumulate in any region of the brain that has been reported to express dopamine D_4 receptors, it accumulated to saturable levels in the posterior eye in the region of retina. This is consistent with the reported high density of dopamine D_4 receptors (B_{max} = 134 fmol·(mg of protein)$^{-1}$) determined by in situ autoradiography with the D_4-selective ligand [^{125}I]L-750,667.[27] The presence of the radioligand in the region of the retina suggests that the compound was able to cross the blood−retina barrier, and therefore, it also has the potential to cross the BBB because it has been reported that both barriers display very similar properties.[55] Moreover, the lack of a persistent signal in other CNS structures indicates that [^{11}C]**7** undergoes a rapid wash-out from the tissues in which it is not significantly bound to the D_4 receptor. It also demonstrates that [^{11}C]**7** has very low nonspecific binding or off-target binding characteristics. This behavior suggests that labeling of lower density brain regions would require a D_4 ligand having an in vitro affinity higher than that of **7** (K_i = 1.52 nM).

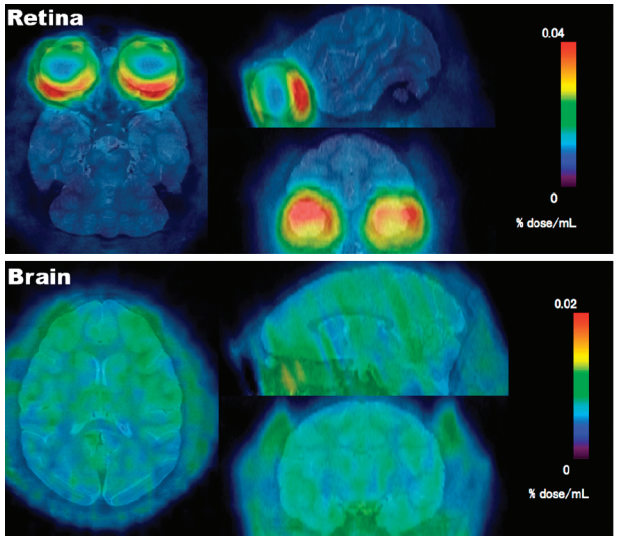

Figure 3. PET imaging in rhesus monkey with [^{11}C]**7** reveals time dependent and saturable binding that is most intense in the posterior regions of the eye. Importantly, there is an intense signal in the region of the retina with little or no background signal in other parts of the CNS. Note different scales used to capture data for retina and brain. Mean images of [^{11}C]**7** from 30 to 90 min after ligand injection are shown.

Conclusions

We report here on a systematic strategy for discovering ligands suitable as PET radiotracers for imaging of dopamine D_4 the receptor in the CNS. Starting from our high-affinity ligand **2** and guided in part by previous structure−activity relationship studies from our laboratories and other laboratories, we developed an assay cascade leading to the design of a set of compounds possessing chemical features amenable to carbon-11 or fluorine-18 labeling and calculated log P values within the range that is considered optimal for a radiotracer. The log P values of the target compounds were determined experimentally confirming that almost all the compounds possessed the desired lipophilicity. Affinity screening of compounds at the dopamine D_4 receptor as well as at selected other off-target receptors (dopamine D_2, dopamine D_3, serotonin 5-HT_{1A}, 5-HT_{2A}, 5-HT_{2C}, σ_1, and cannabinoid CB_1) guided our selection of two potent and selective ligands, namely, *N*-[2-[4-(3-cyanopyridin-2-yl)piperazin-1-yl]ethyl]-3-methoxybenzamide (**7**) and *N*-[2-[4-(3-cyanopyridin-2-yl)piperazin-1-yl]ethyl]-4-fluorobenzamide (**13**). Compounds **7** and **13** showed K_i values of 1.52 and 0.93 nM, respectively, and >100-fold selectivity over the off-target receptors. When tested in disposition studies in mice to evaluate their BBB penetrance and first-pass metabolism characteristics, both **7** and **13** rapidly entered the brain and, importantly in this context, were also rapidly cleared from the brain. Carbon-11 radiolabeling of the phenol precursor **19** resulted in the 3-methoxybenzamide

derivative [^{11}C]**7**. [^{11}C]**7** was injected into rhesus monkey, and brain penetrance as well as its fast washout was confirmed in this non-human primate. Despite there being no labeling of dopamine D_4 receptor in the brain regions examined, [^{11}C]**7** did accumulate in a time-dependent and saturable fashion in the posterior eye in the region of the retina, a CNS tissue rich in dopamine D_4 receptors. While more questions may need to be answered and further improvements could be made, we believe that **7** represents a significant step forward in the development of a CNS PET tracer selective for the dopamine D_4 receptor, having allowed for the first time CNS imaging of D_4 receptor in a structure with the highest known density of this receptor subtype. Importantly, the strategy we worked out appears to serve as a suitable paradigm for developing additional D_4-selective PET tracers which would have higher affinity presumably making them suitable for imaging in brain regions having a very low density of the D_4 receptor. Finally, because of its high affinity and specificity, compound **7** in the tritiated form may have utility as a radioligand for studying the distribution and density of the dopamine D_4 receptor protein in ex vivo or in vitro studies.

Experimental Section

Chemistry. The purity of the tested compounds **2**, **4**−**14** has been assessed by RP-HPLC and combustion analysis. All compounds showed ≥95% purity. Column chromatography was performed with 1:30 Merck silica gel 60A (63−200 μm) as the stationary phase. Melting points were determined in open capillaries on a Gallenkamp electrothermal apparatus. Elemental analyses (C, H, N) were performed on Eurovector Euro EA 3000 analyzer; the analytical results were within ±0.4% of the theoretical values for the formula given. ^{1}H NMR spectra were recorded at 300 MHz on a Varian Mercury-VX spectrometer. All spectra were recorded on free bases. All chemical shift values are reported in ppm (δ). Recording of mass spectra was done on an HP6890-5973 MSD gas chromatograph/mass spectrometer; only significant *m*/*z* peaks, with their percentage of relative intensity in parentheses, are reported. ESI$^+$-MS/MS analysis were performed with an Agilent 1100 series LC-MSD trap system VL workstation. All spectra were in accordance with the assigned structures. RP-HPLC analysis was performed on a Perkin-Elmer series 200 LC instrument using a Phenomenex Gemini RP-18 column, (250 mm × 4.6 mm, 5 μm particle size) and equipped with a Perkin-Elmer 785A UV/vis detector setting of λ = 254 nm. Compounds **2** and **4**−**14** were eluted with $CH_3OH/H_2O/Et_3N$, 4:1:0.01, v/v at a flow rate of 1 mL/min. When necessary, a standard procedure was used to transform final compounds into their hydrochloride salts. The following compounds were synthesized according to published procedures: 1-(4-chloro-2-pyridinyl)-piperazine,[45] 1-(3-cyano-2-pyridinyl)piperazine,[56] 4-(4-chlorophenyl)-1-piperazinoethanamine (**18a**),[44] 4-(4-methylphenyl)-1-piperazinoethanamine (**18b**).[44] The NMR and MS spectra of compounds **2**, **4**, and **8** have been reported earlier.[42,46]

3-[4-(2-Hydroxyethyl)-1-piperazinyl]-1,2-benzisoxazole (15c). A solution of 3-(1-piperazinyl)-1,2-benzisoxazole (0.6 g, 2.96 mmol) in dioxane (15 mL) was treated with anhydrous K_2CO_3 (1.43 g, 10.3 mmol) and KI (0.04 g, 0.2 mmol). After addition of 2-bromoethanol (1.2 mL, 17.3 mmol) the mixture was refluxed overnight. The solvent was distilled off, and the residue was partitioned between H_2O (20 mL) and $CHCl_3$ (20 mL). The organic phase was separated, dried over anhydrous Na_2SO_4, and concentrated under reduced pressure. The crude residue was chromatographed ($CHCl_3$/MeOH 19:1, as eluent) to afford the pure alcohol as a white solid (0.56 g, 77% yield). ^{1}H NMR ($CDCl_3$): δ 2.10 (br s, 1H, D_2O exchanged), 2.64 (t, 2H, *J* = 5.5 Hz), 2.73 (app t, 4H), 3.60 (app t, 4H), 3.68 (t, 2H, *J* = 5.5 Hz), 7.20−7.24 (m, 1H), 7.44−7.49 (m, 2H), 7.69 (d, 1H, *J* = 8.0 Hz). ESI$^+$-MS *m*/*z* 248.2 (MH^+). ESI$^+$-MS/MS *m*/*z* 161.2 (100), 114.4 (22).

4-[4-(2-Hydroxyethyl)-1-piperazinyl]benzonitrile (15d). A stirred mixture of 4-piperazinobenzonitrile (0.37 g, 2.0 mmol), 2-chloroethanol (0.17 mL, 2.4 mmol), and K_2CO_3 (0.35 g, 2.5 mmol) in acetonitrile was refluxed overnight. After cooling, the mixture was evaporated to dryness and H_2O (20 mL) was added to the residue. The aqueous phase was extracted with CH_2Cl_2 (2 × 20 mL). The collected organic layers were dried over Na_2SO_4 and evaporated under reduced pressure. The crude residue was chromatographed ($CHCl_3/CH_3OH$, 19:1 as eluent) to yield pure **15d** as a white solid (0.30 g, 64% yield). ^{1}H NMR ($CDCl_3$): δ 1.71 (br s, 1H, D_2O exchanged), 2.61 (t, 2H, *J* = 5.5 Hz), 2.65 (app t, 4H), 3.34 (app t, 4H), 3.67 (t, 2H, *J* = 5.5 Hz), 6.83−6.88 (m, 2H), 7.47−7.52 (m, 2H). GC−MS *m*/*z* 232 ($M^+ + 1$, 5), 231 (M^+, 17), 200 (100), 157 (24), 129 (24).

3-Cyano-2-[4-(2-hydroxyethyl)-1-piperazinyl]pyridine (15e). Title compound was prepared from 1-(3-cyano-2-pyridyl)piperazine and 2-chloroethanol following the same procedure described above for **15d**. Pure **15e** was obtained by column chromatography ($CHCl_3$/CH_3OH, 19:1, as eluent) as a yellow oil in 83% yield. ^{1}H NMR ($CDCl_3$): δ 2.51 (br s, 1H, D_2O exchanged), 2.75 (t, 2H, *J* = 5.3 Hz), 2.83 (app t, 4H), 3.76 (t, 2H, *J* = 5.3 Hz), 3.83 (app t, 4H), 6.80 (q, 1H, *J* = 7.4, 7.7 Hz), 7.79 (dd, 1H, *J* = 1.9, 7.7 Hz), 8.34−8.37 (m, 1H). GC−MS *m*/*z* 233 ($M^+ + 1$, 1), 232 (M^+, 5), 201 (100), 172 (47), 146 (46), 100 (40).

General Procedure for Preparation of Compounds 16c−e. Diethyl azodicarboxylate (2.25 mmol) was added to a stirred solution containing the appropriate alcohol **15c**−**e** (1.5 mmol), triphenylphosphine (1.5 mmol), and phthalimide (2.25 mmol) in anhydrous THF (20 mL). The resulting mixture was stirred at room temperature under anhydrous condition until the alcohol disappeared (TLC). Then the mixture was partitioned between AcOEt (20 mL) and H_2O (20 mL). The organic layer was separated, dried (Na_2SO_4), and concentrated in vacuo. The crude residue was chromatographed as detailed below to afford pure compounds as pale yellow solids in quantitative yield.

2-[2-[4-(1,2-Benzisoxazol-3-yl)-1-piperazinyl]ethyl]-1*H*-isoindole-1,3(2*H*)-dione (16c). Eluted with $CHCl_3$/AcOEt, 1:1. ^{1}H NMR ($CDCl_3$): δ 2.69−2.74 (m, 6H), 3.50 (app t, 4H), 3.86 (t, 2H, *J* = 6.4 Hz), 7.20 (dtd, 1H, *J* = 1.6, 6.3, 8.1 Hz), 7.43−7.49 (m, 2H), 7.66−7.74 (m, 3H), 7.83−7.85 (m, 2H). ESI$^+$-MS *m*/*z* 377.1 (MH^+). ESI$^+$-MS/MS *m*/*z* 174.2 (100), 147.3 (24).

2-[2-[4-(4-Cyanophenyl)-1-piperazinyl]ethyl]-1*H*-isoindole-1,3-(2*H*)-dione (16d). Eluted with $CHCl_3$/AcOEt, 9:1. ^{1}H NMR ($CDCl_3$): δ 2.64 (app t, 4H), 2.69 (t, 2H, *J* = 6.3 Hz), 3.24 (app t, 4H), 3.85 (t, 2H, *J* = 6.3 Hz), 6.80−6.84 (m, 2H), 7.45−7.48 (m, 2H), 7.71−7.73 (m, 2H), 7.83−7.85 (m, 2H). GC−MS *m*/*z* 361 ($M^+ + 1$, 1), 360 (M^+, 1), 200 (100), 157 (17).

2-[2-[4-(3-Cyanopyridin-2-yl)-1-piperazinyl]ethyl]-1*H*-isoindole-1,3(2*H*)-dione (16e). Eluted with $CHCl_3$/AcOEt, 1:1. ^{1}H NMR ($CDCl_3$): δ 2.66 (app t, 4H), 2.69 (t, 2H, *J* = 6.3 Hz), 3.66 (app t, 4H), 3.85 (t, 2H, *J* = 6.3 Hz), 6.71 (q, 1H, *J* = 7.7 Hz), 7.70−7.75 (m, 3H), 7.82−7.86 (m, 2H), 8.31 (dd, 2H, *J* = 1.9, 5.0 Hz). GC−MS *m*/*z* 362 ($M^+ + 1$, 1), 361 (M^+, 4), 242 (19), 201 (100), 172 (19).

4-(5-Chloropyridin-2-yl)piperazinoacetonitrile (17). A stirred mixture of 1-(5-chloropyridin-2-yl)piperazine (2.25 g, 11.4 mmol), chloroacetonitrile (0.60 mL, 9.5 mmol), and an excess of K_2CO_3 in acetonitrile (50 mL) was refluxed overnight. After cooling, the mixture was evaporated to dryness. Then H_2O was added to the residue. The aqueous phase was extracted with CH_2Cl_2 (2 × 30 mL), and the collected organic layers were dried over Na_2SO_4 and evaporated under reduced pressure. The crude residue was chromatographed ($CHCl_3$/AcOEt, 9:1, as eluent) to give pure **17** as a pale yellow semisolid (2.0 g, 90% yield). ^{1}H NMR ($CDCl_3$): δ 2.69 (app t, 4H), 3.55−3.59 (m, 6H), 6.59 (dd, 1H, *J* = 0.5, 9.1 Hz), 7.43 (dd, 1H, *J* = 2.5, 9.1 Hz), 8.11 (dd, 1H, *J* = 0.5, 2.5 Hz). GC−MS *m*/*z* 238 ($M^+ + 2$, 9), 236 (M^+, 27), 143 (33), 141 (100), 113 (21).

General Procedure for Preparation of Amines 18c−e. Phthalimide derivative **16c**−**e** (1.5 mmol) was mixed with an excess of

hydrazine hydrate in EtOH (20 mL) and refluxed for 8 h. Then the mixture was cooled on ice bath and acidified with concentrated HCl. The mixture was refluxed for 1 h. Then the mixture was cooled and filtered. The filtrate was concentrated under reduced pressure, and the residue was partitioned between 10% aqueous NaOH and $CHCl_3$. The separated organic layer was dried over Na_2SO_4 and concentrated in vacuo to give the pure amine in 70−80% yield.

4-(1,2-Benzisoxazol-3-yl)-1-piperazinoethanamine (18c). ^{1}H NMR ($CDCl_3$): δ 1.72 (br s, 2H, D_2O exchanged), 2.50 (t, 2H, J = 6.0 Hz), 2.65 (app t, 4H), 2.83 (t, 2H, J = 6.0 Hz), 3.58 (app t, 4H), 7.20 (dtd, 1H, J = 1.6, 6.2, 8.0 Hz), 7.42−7.50 (m, 2H), 7.68 (d, 1H, J = 8.3 Hz). ESI$^+$-MS m/z 247.2 (MH^+). ESI$^+$-MS/MS m/z 230.2 (100).

4-(4-Cyanophenyl)-1-piperazinoethanamine (18d). ^{1}H NMR ($CDCl_3$): δ 1.83 (br s, 2H, D_2O exchanged), 2.47 (t, 2H, J = 6.0 Hz), 2.58 (app t, 4H), 2.82 (t, 2H, J = 6.3 Hz), 3.32 (app t, 4H), 6.82−6.88 (m, 2H), 7.45−7.50 (m, 2H). GC−MS m/z 231 (M^+ + 1, 1), 230 (M^+, 3), 200 (100), 157 (33), 70 (34).

4-(3-Cyanopyridin-2-yl)-1-piperazinoethanamine (18e). ^{1}H NMR ($CDCl_3$): δ 1.75 (br s, 2H, D_2O exchanged), 2.48 (t, 2H, J = 6.1 Hz), 2.59 (app t, 4H), 2.82 (t, 2H, J = 6.3 Hz), 3.73 (app t, 4H), 6.73 (q, 1H, J = 7.4, 7.7 Hz), 7.75 (dd, 1H, J = 1.9, 7.6 Hz), 8.32 (dd, 1H, J = 1.9, 4.7 Hz). GC−MS m/z 232 (M^+ + 1, 1), 231 (M^+, 1), 201 (100), 172 (37), 146 (36).

4-(5-Chloropyridin-2-yl)piperazineethanamine (18f). Borane−methyl sulfide complex as 10.0 M BH_3 in excess methyl sulfide (1.6 mL, 16 mmol) was dropped into an ice cooled solution of nitrile **17** (5.1 mmol) in anhydrous THF (10 mL), under stirring. After being refluxed for 4 h, the reaction mixture was cooled at −10 °C and MeOH was added dropwise very carefully until gas evolution ceased. The mixture was treated with 3 N HCl (20 mL) and was refluxed for 1 h. After cooling, the mixture was alkalized with 3 N NaOH and extracted with CH_2Cl_2 (2 × 30 mL). The collected organic layers were dried over Na_2SO_4 and the solvent was evaporated under reduced pressure to give the pure amine as a white semisolid (64% yield). ^{1}H NMR ($CDCl_3$): δ 1.73 (br s, 2H, D_2O exchanged), 2.46 (t, 2H, J = 6.1 Hz), 2.54 (app t, 4H), 2.82 (app t, 2H), 3.50 (app t, 4H), 6.57 (d, 1H, J = 9.1 Hz), 7.40 (dd, 1H, J = 2.5, 9.1 Hz), 8.09 (d, 1H, J = 2.5 Hz). GC−MS m/z 242 (M^+ + 2, 1), 240 (M^+, 4), 212 (33), 210 (100), 181 (57), 155 (62), 112 (33).

General Procedure for Preparation of Compounds 5−7, 9−14, 19. A mixture of the appropriate benzoic acid (0.48 mmol) and 1,1′-carbonyldiimidazole (0.50 mmol) in 10 mL of anhydrous THF was stirred for 8 h. A solution of amine **18a−f** (0.48 mmol) in anhydrous THF (10 mL) was added, and then the mixture was stirred until the benzoic acid disappeared (TLC). The reaction mixture was partitioned between AcOEt (20 mL) and H_2O (20 mL). The separated organic layer was washed with a saturated aqueous solution of Na_2CO_3 (20 mL), dried (Na_2SO_4), and concentrated in vacuo. The crude residue was chromatographed as detailed below to afford the pure arylcarboxamide in 40−50% yield.

***N*-[2-[4-(1,2-Benzisoxazol-3-yl)piperazin-1-yl]ethyl]-3-methoxybenzamide (5).** Eluted with $CHCl_3$/MeOH, 98:2. ^{1}H NMR ($CDCl_3$): δ 2.73 (t, 2H, J = 5.5 Hz), 2.77 (app t, 4H), 3.60−3.65 (m, 6H), 3.84 (s, 3H), 6.95 (br s, 1H, D_2O exchanged), 7.03 (dt, 1H, J = 2.5, 6.9 Hz), 7.20−7.22 (m, 2H), 7.23−7.26 (m, 1H), 7.29−7.34 (m, 1H), 7.37−7.52 (m, 2H), 7.66−7.69 (m, 1H). ESI$^+$-MS m/z 381.0 (MH^+). ESI$^+$-MS/MS m/z 178.2 (100). The hydrochloride salt melted at 202−204 °C (from MeOH/Et_2O). Anal. ($C_{21}H_{24}N_4O_3 \cdot HCl \cdot H_2O$) C, H, N.

***N*-[2-[4-(4-Cyanophenyl)piperazin-1-yl]ethyl]-3-methoxybenzamide (6).** Eluted with $CHCl_3$/MeOH, 19:1. ^{1}H NMR ($CDCl_3$): δ 2.66−2.70 (m, 6H), 3.36 (app t, 4H), 3.60 (q, 2H, J = 5.5 Hz), 3.84 (s, 3H), 6.79 (br s, 1H, D_2O exchanged), 6.84−6.89 (m, 2H), 7.03 (dq, 1H, J = 1.1, 1.4, 8.0 Hz), 7.26−7.38 (m, 3H), 7.47−7.52 (m, 2H). GC−MS m/z 364 (M^+, 2), 213 (16), 200 (100), 157 (21). Mp 174−175 °C (from $CHCl_3$/*n*-hexane). Anal. ($C_{21}H_{24}N_4O_2$) C, H, N.

***N*-[2-[4-(3-Cyanopyridin-2-yl)piperazin-1-yl]ethyl]-3-methoxybenzamide (7).** Eluted with $CHCl_3$/AcOEt, 1:1. ^{1}H NMR ($CDCl_3$): δ 2.67−2.71 (m, 6H), 3.60 (q, 2H, J = 5.3 Hz), 3.76 (app t, 4H), 3.85 (s, 3H), 6.77 (dd, 1H, J = 4.7, 7.7 Hz), 6.85 (br s, 1H, D_2O exchanged), 7.02−7.05 (m, 1H), 7.26−7.38 (m, 3H), 7.77 (dd, 1H, J = 1.1, 8.7 Hz), 8.35 (dd, 1H, J = 1.1, 3.7 Hz). GC−MS m/z 366 (M^+ + 1, 1), 365 (M^+, 2), 201 (100), 146 (18). The hydrochloride salt melted at 180 °C dec (from MeOH/Et_2O). Anal. ($C_{20}H_{23}N_5O_2 \cdot 2HCl$) C, H, N.

***N*-[2-[4-(4-Chlorophenyl)piperazin-1-yl]ethyl]-4-fluorobenzamide (9).** Eluted with $CHCl_3$/MeOH, 19:1. ^{1}H NMR ($CDCl_3$): δ 2.72−2.76 (m, 6H), 3.23 (app t, 4H), 3.62 (q, 2H, J = 5.3 Hz), 6.81−6.87 (m, 2H), 6.99 (br s, 1H, D_2O exchanged), 7.07−7.15 (m, 2H), 7.18−7.24 (m, 2H), 7.79−7.85 (m, 2H). GC−MS m/z 363 (M^+ + 2, 3), 361 (M^+, 8), 211 (32), 209 (100), 166 (23). Mp 180−181 °C (from $CHCl_3$/*n*-hexane). Anal. ($C_{19}H_{21}FClN_3O$) C, H, N.

***N*-[2-[4-(4-Methylphenyl)piperazin-1-yl]ethyl]-4-fluorobenzamide (10).** Eluted with $CHCl_3$/MeOH, 19:1. ^{1}H NMR ($CDCl_3$): δ 2.27 (s, 3H), 2.71−2.76 (m, 6H), 3.22 (app t, 4H), 3.62 (q, 2H, J = 5.5 Hz), 6.83−6.87 (m, 2H), 7.00 (br s, 1H, D_2O exchanged), 7.01−7.14 (m, 4H), 7.79−7.85 (m, 2H). GC−MS m/z 342 (M^+ + 1, 3), 341 (M^+, 13), 189 (100), 123 (22). Mp 156−158 °C (from $CHCl_3$/*n*-hexane). Anal. ($C_{20}H_{24}FN_3O$) C, H, N.

***N*-[2-[4-(1,2-Benzisoxazol-3-yl)piperazin-1-yl]ethyl]-4-fluorobenzamide (11).** Eluted with $CHCl_3$/MeOH, 98:2. ^{1}H NMR ($CDCl_3$): δ 2.74−2.82 (m, 6H), 3.61−3.68 (m, 6H), 6.93 (br s, 1H, D_2O exchanged), 7.03−7.15 (m, 2H), 7.19−7.24 (m, 1H), 7.44−7.53 (m, 2H), 7.67 (d, 1H, J = 8.0 Hz) 7.80−7.87 (m, 2H). ESI$^+$-MS m/z 369.1 (MH^+). ESI$^+$-MS/MS m/z 166.2 (100). Mp 138−140 °C (from $CHCl_3$/*n*-hexane). Anal. ($C_{20}H_{21}FN_4O_2$) C, H, N.

***N*-[2-[4-(4-Cyanophenyl)piperazin-1-yl]ethyl]-4-fluorobenzamide (12).** Eluted with $CHCl_3$/MeOH, 19:1. ^{1}H NMR ($CDCl_3$): δ 2.70−2.72 (m, 6H), 3.39 (app t, 4H), 3.59−3.65 (m, 2H), 6.84−6.89 (m, 2H), 6.93 (br s, 1H, D_2O exchanged), 7.07−7.15 (m, 2H), 7.48−7.52 (m, 2H), 7.78−7.83 (m, 2H). GC−MS m/z 353 (M^+ + 1, 1), 351 (M^+, 2), 200 (100), 157 (20). Mp 193−194 °C (from $CHCl_3$/*n*-hexane). Anal. ($C_{20}H_{21}FN_4O$) C, H, N.

***N*-[2-[4-(3-Cyanopyridin-2-yl)piperazin-1-yl]ethyl]-4-fluorobenzamide (13).** Eluted with $CHCl_3$/MeOH, 19:1. ^{1}H NMR ($CDCl_3$): δ 2.78 (br s, 6H), 3.62−3.67 (m, 2H), 3.82 (app t, 4H), 6.80 (q, 1H, J = 7.4, 7.7 Hz), 6.93 (br s, 1H, D_2O exchanged), 7.08−7.16 (m, 2H), 7.79 (dd, 1H, J = 1.9, 7.4 Hz), 7.82−7.87 (m, 2H), 8.36 (dd, 1H, J = 1.9, 5.0 Hz). GC−MS m/z 354 (M^+ + 1, 1), 353 (M^+, 1), 201 (100), 123 (22). Mp 155−156 °C (from $CHCl_3$/*n*-hexane). Anal. ($C_{19}H_{20}FN_5O$) C, H, N.

***N*-[2-[4-(5-Chloropyridin-2-yl)piperazin-1-yl]ethyl]-4-fluorobenzamide (14).** Eluted with $CHCl_3$/MeOH, 19:1. ^{1}H NMR ($CDCl_3$): δ 2.65−2.72 (m, 6H), 3.56−3.64 (m, 6H), 6.59 (d, 1H, J = 9.1 Hz), 6.93 (br s, 1H, D_2O exchanged), 7.07−7.15 (m, 2H), 7.43 (dd, 1H, J = 2.8, 9.1 Hz), 7.78−7.84 (m, 2H), 8.11 (d, 1H, J = 2.5 Hz). GC−MS m/z 364 (M^+ + 2, 1), 362 (M^+, 3), 210 (100), 181 (34), 155 (40), 123 (52). Mp 173−175 °C (from $CHCl_3$/*n*-hexane). Anal. ($C_{18}H_{20}FClN_4O$) C, H, N.

***N*-[2-[4-(3-Cyanopyridin-2-yl)piperazin-1-yl]ethyl]-3-hydroxybenzamide (19).** Eluted with AcOEt. ^{1}H NMR ($CDCl_3$): δ 2.67−2.71 (m, 6H), 3.56−3.62 (m, 2H), 3.76 (app t, 4H), 6.75−6.79 (m, 1H), 6.96 (br s, 1H, D_2O exchanged), 6.97−6.99 (m, 1H), 7.18−7.24 (m, 2H), 7.48 (m, 1H), 7.78 (dd, 1H, J = 1.9, 7.4 Hz), 8.35 (dd, 1H, J = 1.9, 4.7 Hz). ESI$^+$-MS m/z 352.1 (MH^+). ESI$^+$-MS/MS m/z 164.2 (100), 121.2 (15).

Lipophilicity Data. Lipophilicity data of compounds **2** and **4−13** were obtained by the pH metric technique using a GlpK_a apparatus (Sirius Analytical Instruments Ltd., Forrest Row, East Sussex, United Kingdom) as described elsewhere.[57] The low aqueous solubility of the investigated compounds required pK_a measurements to be performed in the presence of methanol as cosolvent. Three separate 20 mL semiaqueous solutions of approximately 5×10^{-5} M, in 20−50% w/w of MeOH, were initially acidified with 0.5 M HCl to pH 3.5. The solutions were then titrated with 0.5 M KOH to pH 11. The initial estimates of

Table 5. Radioligand and Drugs Used to Define Nonspecific Binding for Each of the Receptor Subtypes Tested[a]

receptor	radioligand	drug for defining nonspecific binding	binding buffer	binding conditions
5-HT_{1A}	[^{3}H]MPPF	NAN-190	50 mM Tris, pH 7.4 at 25 °C	90 min at 25 °C
5-HT_{2A}	[^{3}H]MSP	mianserin	50 mM Tris, pH 7.4 at 25 °C	90 min at 25 °C
5-HT_{2C}	[^{3}H]mesulergine	mianserin	50 mM Tris, pH 7.4 at 25 °C	90 min at 25 °C
D_2	[^{3}H]MSP	(+)-butaclamol	50 mM Tris, pH 7.4 at 25 °C	90 min at 25 °C
D_3	[^{3}H]MSP	7-OH-DPAT	50 mM Tris, pH 7.4 at 25 °C	90 min at 25 °C
D_4	[^{3}H]MSP	(+)-butaclamol	50 mM Tris, pH 7.4 at 25 °C	90 min at 25 °C
σ_1	[^{3}H]-(+)-pentazocine	BD1063	50 mM Tris, pH 8.0 at 37 °C	180 min at 37 °C with shaking
CB_1	[^{3}H]CP55,940	O-2050	50 mM Tris, pH 7.4 at 30 °C, 2.5 mM EDTA, 5 mM $MgCl_2$, 5 mg/mL fatty acid free BSA	180 min at 30 °C with shaking

[a] [^{3}H]MPPF is 4-(2″-methoxy)phenyl-1-[2″-(*N*-2-pyridinyl)-*p*-fluorobenzamido]ethylpiperazine (Perkin Elmer, St. Louis, MO, NET-1109, 80 Ci/mmol). [^{3}H]MSP is [^{3}H]methylspiperone (Perkin Elmer, St. Louis, MO, NET-856, 84 Ci/mmol). [^{3}H]mesulergine (GE Healthcare Life Sciences, Piscataway, NJ, TRK845, 80 Ci/mmol). [^{3}H]-(+)-pentazocine (Perkin Elmer, St. Louis, MO, NET1056, 29 Ci/mmol). [^{3}H]CP55,940 (Perkin Elmer, St. Louis, MO, NET1051, 180 Ci/mmol). Note that all radioligands were tested at approximately 0.5 pM, except for [^{3}H]-(+)-pentazocine and [^{3}H]CP55,940, which were tested at 1 and 2 nM, respectively. A concentration of 5 μM was used to define nonspecific binding for all receptors.

the p_sK_a values, which are the apparent ionization constants in the mixed solvent, were obtained by Bjerrum plots. These values were then refined by a weighted nonlinear least-squares procedure (Refinement Pro 1.0 software) to create a multiset, where the refined values were extrapolated to zero cosolvent concentration using the Yasuda−Shedlovsky equation.[58] To obtained log *P* data, at least three separate titrations were performed on each compound, of approximately 5×10^{-5} M, using various *n*-octanol/water ratios (from 0.005 to 1). The biphasic solutions were initially acidified to pH 3.5 with 0.5 M HCl and then titrated with 0.5 M KOH to pH 11. The obtained data were refined as described above. The log *P* values were obtained by the multiset approach, as described elsewhere.[57] All titrations were carried out at 25 ± 0.1 °C under an inert nitrogen gas atmosphere to exclude CO_2.

Radiosynthesis of [^{11}C]7. Carbon-11 was produced by ^{14}N(p, α)^{11}C nuclear reaction using CYPRIS HM-18 cyclotron (Sumitomo Heavy Industry Co. Ltd., Tokyo, Japan). [^{11}C]CH_3I with high specific activity was produced by the single-pass I_2 method as described previously.[59] By the nuclear reaction and a successive hot atom process, [^{11}C]CH_4 (total radioactivity: 44 GBq) was produced in the target chamber at an initial pressure of 15 bar with 18 MeV protons (14.2 Mev on target). [^{11}C]CH_4 was passed through a heated I_2 column once and converted to [^{11}C]CH_3I, which was collected in a reaction vessel containing a 300 μL of anhydrous DMF solution of desmethyl precursor **19** (1 mg) and NaOH (10 μL, 0.5 N) at −15 to −20 °C. After radioactivity reached a plateau, the reaction mixture was heated at 70 °C for 3 min. The HPLC solvent was added to the reaction vessel to terminate the reaction. The radioactive mixture was applied to an HPLC purification system (SHISEIDO CAPCELL PAK C18 UG80 column, 10 mm × 250 mm; mobile phase CH_3OH/H_2O/triethylamine, 6/4/0.1%; flow rate, 5 mL/min; λ = 254 nm). The fraction corresponding to [^{11}C]**7** was collected in a flask containing 100 μL of ascorbic acid (25%) and evaporated to dryness under a vacuum. The residue was dissolved in 3 mL of saline (pH 7.4) for animal experiments. At the end of synthesis, 210−440 MBq (n = 4) of [^{11}C]**7** was obtained as an intravenous injectable solution. The radiochemical purity and specific activity of [^{11}C]**7** were assayed by analytical HPLC (SHISEIDO CAPCELL PAK C18 UG80 column, 10 mm × 250 mm; mobile phase CH_3OH/H_2O/triethylamine, 6/4/0.1%; flow rate, 5 mL/min; λ = 254 nm). The identity of [^{11}C]**7** was confirmed by coinjection with an authentic nonradioactive sample. The amount of carrier in the final product solution was measured by the same analytical HPLC. The radiochemical purity and specific activity was >99% and 2770−3890 GBq/μmol (n = 4), respectively.

Biological Methods. 1. Preparation of Crude Membranes for Binding Assays. A human embryonic kidney cell line (HEK293) was employed as the host cell for expressing individually the cloned rat dopamine D_2 and D_4 receptors and human serotonin 5-HT_{1A}, 5-HT_{2A}, and 5-HT_{2C} receptors because all these receptor subtypes are absent in HEK293 cells; i.e., HEK293 cells lack specific binding for the radioligands used to characterize each of the receptor subtypes (data not shown). HEK293 cell lines stably expressing high levels of D_2, D_4, 5-HT_{1A}, 5-HT_{2A}, or 5-HT_{2C} receptors were created as described by us previously.[60−62] The expression levels of the different receptor subtypes in individual clonal lines were determined by radioligand saturation isotherm binding utilizing standard rapid filtration techniques and cell membrane preparations as described by us previously.[63] Cloned human σ_1 receptors were stably expressed in human MCF-7 cells as described by us previously, because MCF-7 cells lack specific binding for [^{3}H]-(+)-pentazocine, the radioligand used to characterize σ_1 receptor binding potential.[48] The membranes from these σ_1-expressing MCF-7 cells were prepared as described previously.[48] With the exception of membranes containing D_3 receptors, all membranes isolated from clonal cell lines were placed in their respective binding buffers (Table 5) and kept on ice until use that same day. Frozen membranes from CHO-K1 cells containing the human dopamine D_3 receptor were purchased from Perkin-Elmer Life Science.

Whole rat brains with the cerebellum and brain stem removed were used as the tissue source for rat cannabinoid CB_1 receptors. Briefly, two to three stripped and frozen Sprague−Dawley rat brains (Pel Freeze Bio, 56005-2) were allowed to slow-thaw by incubating on ice in 30 mL of cold 20 mM Tris, pH 7.4, at 2 °C and 1:1000 v/v diluted protease inhibitor cocktail (Sigma-Aldrich, P8340). Thawed brains were homogenized with 10 strokes in a Dounce glass−glass homogenizer and the suspension was centrifuged for 10 min at 1000*g* (Sorvall Legend RT). The resulting supernatant was transferred to a new tube and centrifuged for 1 h at 4 °C at 25000*g* (Sorvall RC-5). The supernatant was discarded and the pellet resuspended in 5 mL of cold 20 mM Tris, pH 7.4, at 2 °C and rehomogenized with four strokes. The homogenate was separated into 1 mL aliquots in cryotubes and stored in liquid nitrogen until use at a 1:5 v/v dilution in binding buffer (see Table 5).

2. Radioligand Binding Assays. Compounds were tested for their ability to compete with radioligands specifically bound to membranes from cells or tissues expressing the dopamine D_2 or D_3 or D_4 receptors, serotonin 5-HT_{1A}, 5-HT_{2A}, or 5-HT_{2C} receptors, σ_1 receptors, and cannabinoid CB_1 receptors. The radioligands and drugs used to define nonspecific binding to each receptor system are shown in Table 5. All binding reactions were allowed to reach equilibrium prior to rapid filtration. Glass tubes were used in all binding reactions except those for cannabinoid receptors which utilized silanized glass tubes. Binding reactions were rapidly terminated by filtration through GF/C filters pretreated with 0.5% polyethyleneimine, or GF/B filter pretreated with 1% polyethyleneimine in the case of cannabinoid receptors, and washing with 3 × 3 mL of ice-cold (0−2 °C)

binding buffer at the pH at that temperature. Radioactivity bound to filters was quantified in a scintillation counter. Membrane protein concentrations were determined using the bicinchonic acid protein reagent (BCA) and a bovine serum albumin standard curve. Membranes protein concentrations varied from 0.01 to 0.05 mg/mL. Binding affinities (K_i) were determined by competition binding with fixed concentrations of the radioligands described in Table 5. With the exception of **6**, **7**, and **12**, which were dissolved in DMF, all compounds were solubilized in DMSO at concentrations ranging from 1 to 10 mM. These nonaqueous solution stocks were then diluted at least 1:1000 v/v in the final assay solution.

3. Calculations and Data Analysis. All points were run in triplicate. Each experiment was repeated three to four times, and averaged values were reported with their standard deviation or standard error. The inhibition constant (K_i) values were calculated from IC_{50} values using the Cheng−Prusoff equation: $K_i = IC_{50}/(1 + [\text{ligand}]/K_D)$.[64] In cases where the displacement was >20% but less than 100% at the highest concentration of inhibitor, the bottom of the curve fit was set to zero so that accurate IC_{50} values could be calculated. A 95% confidence interval was employed for all curve-fitting procedures using Graphpad's Prism software, version 4.0.

4. Preliminary Disposition Studies. Male CD1 mice weighing 25−30 g (Charles River, Italy) were administered compounds **7** or **13** (10 mg/kg ip, dissolved in ethanol/PEG 40/saline (10:40:50, v/v) and were sacrificed by decapitation at 15, 30, 60, 120, and 240 min after dosing to determine the plasma and brain concentrations of the parent compounds and their potential metabolite 1-(6-cyano-2-pyridyl)piperazine. Procedures involving animals and their care were conducted in conformity with the institutional guidelines that are in complicance with national (D.L. n. 116, G.U., Suppl. 40, 18 Febbraio 1992, Circolare No. 8, G.U., 14 Luglio 1994) and international laws and policies (EEC Council Directive 86/609, OJ L 358, 1, Dec 12, 1987; Guide for the Care and Use of Laboratory Animals, U.S. National Research Council, 1996). Concentrations of the selected compounds were determined by HPLC with UV detection (λ = 264 nm). Briefly, to 0.2 mL of plasma, 0.01 mL of 1 M NaOH, 0.03 mL of the internal standard 1-(2-thiazolyl)piperazine (10 μg/mL), and 5 mL of dicloromethane were added. After being shaken, samples were centrifuged, and to the organic extract 0.15 mL of mobile phase was added. After further shaking and centrifugation, 0.1 mL of the mobile phase was injected onto the HPLC system. Brains were homogenized in distilled water (1 g/10 mL), and an amount of 2 mL of the homogenate was processed as above. Chromatography was performed on a reversed-phase column XTerra RP 18 (4.6 mm × 150 mm, 5 μm particle size). The mobile phase was CH_3CN/ 0.005 M KH_2PO_4 (pH 3.5) (5:95, v/v) (solvent A) and CH_3CN/ 0.005 M KH_2PO_4 (pH 3.5) (70:30, v/v) (solvent B). The HPLC system was set up to operate at a flow rate of 1 mL/min, following a simple gradient: step 1, from the initial condition (100% solvent A) to 20% solvent A (80% B) in 12 min; step 2, from 20% to 100% solvent A (from 80% to 0% of solvent B) in 2 min. The total run time was 18 min.

The retention times were 8.7 min for **7**, 8.8 for **13**, 4.5 min for 1-(6-cyano-2-pyridyl)piperazine, and 7.7 min for internal standard. The limit of quantification was about 100 ng/mL or ng/g, using 0.2 mL of plasma or about 200 mg of tissue. At these concentrations, the coefficients of variation (CV) were generally between 10% and 15%, and all higher concentrations gave CV between 5% and 10% for all compounds in both tissues.

5. Monkey PET Scan. PET scans were performed on a male rhesus monkey (*Macaca mulatta*) weighing 4.4 kg. The animal was maintained and handled in accordance with recommendations by the U.S. National Institutes of Health and our institutional guidelines (National Institute of Radiological Sciences). The studies were approved by the Animal Ethics Committee of the National Institute of Radiological Sciences, Chiba, Japan. PET scan was performed using a high-resolution SHR-7700 PET camera (Hamamatsu Photonics K.K., Japan) designed for laboratory animals, which provides 31 transaxial slices 3.6 mm (center-to-center) apart, a 33.1 cm field of view, and spatial resolution of 2.6 mm full width at half-maximum.[65] The monkey was anesthetized with ketamine at 10 mg/kg im (Ketalar, Sankyo Co. Ltd., Japan) with a head fixation device to ensure accuracy of repositioning.[66] Following transmission scans for attenuation correction using a $^{68}Ge-^{68}Ga$ source for 20 min, a dynamic emission scan in 3D acquisition mode was immediately performed after intravenous injection of [^{11}C]**7** (38.5 ± MBq; specific radioactivity, 2.9 TBq/μmol at injection) for 90 min (0.5 min × 6 frames, 1 min × 7 frames, 2 min × 20 frames, 5 min × 8 frames). Dynamic emission scan images were reconstructed with filtered back-projection using a 4.0 mm Colsher filter. Volumes of interest (VOIs) were placed on the hippocampus, entorhinal cortex, and striatum using PMOD image analysis software (PMOD Group, Zurich, Switzerland) with reference to the magnetic resonance (MR) image of the monkey brain. The MR image was acquired with a 1.5 T gyroscan S15/ACS2 (Philips Electronic, Eindhoven, The Netherlands) by means of a three-dimensional T_1-weighted spin−echo sequence. The tracer uptake in each VOI was estimated as percent of injected dose per unit volume (% ID/mL).

Acknowledgment. This study was supported by the National Institutes of Health [Grants R01-MH063162 and R01-MH063162-06S1 (J.A.S.)] and the National Science Foundation [DBI-0649889 (J.A.S.)].

Supporting Information Available: Elemental analysis data of target compounds and time−activity data. This material is available free of charge via the Internet at http://pubs.acs.org.

References

(1) Van Tol, H. H.; Bunzow, J. R.; Guan, H. C.; Sunahara, R. K.; Seeman, P.; Niznik, H. B.; Civelli, O. Cloning of the gene for a human dopamine D_4 receptor with high affinity for the antipsychotic clozapine. *Nature* **1991**, *350*, 610–614.

(2) Lahti, R. A.; Evans, D. L.; Stratman, N. C.; Figur, L. M. Dopamine D_4 versus D_2 receptor selectivity of dopamine receptor antagonists: possible therapeutic implications. *Eur. J. Pharmacol.* **1993**, *236*, 483–486.

(3) Zhang, K.; Bardessarini, R. J.; Tarazi, F. I.; Neumeyer, J. L. Selective dopamine D_4 receptor antagonists: review of structure−activity relationships. *Curr. Med. Chem.: Cent. Nerv. Syst. Agents* **2002**, *2*, 259–274.

(4) Bristow, L. J.; Collinson, N.; Cook, G. P.; Curtis, N.; Freedman, S. B.; Kulagowski, J. J.; Leeson, P. D.; Patel, S.; Ragan, C. I.; Ridgill, M.; Saywell, K. L.; Tricklebank, M. L-745,870, a subtype selective dopamine D_4 receptor antagonist, does not exhibit a neuroleptic-like profile in rodent behavioral tests. *J. Pharmacol. Exp. Ther.* **1997**, *283*, 1256–1263.

(5) Kramer, M. S.; Last, B.; Getson, A.; Reines, S. A. The effects of a selective D_4 dopamine receptor antagonist (L-745,870) in acutely psychotic in patients with schizophrenia. D_4 dopamine antagonist group. *Arch. Gen. Psychiatry* **1997**, *54*, 567–572.

(6) Gazi, L.; Bobirnac, I.; Danzeisen, M.; Schupbach, E.; Bruinvels, A. T.; Geisse, S.; Sommer, B.; Hoyer, D.; Tricklebank, M.; Schoeffter, P. The agonist activities of the putative antipsychotic agents, L745,870 and U-101958 in HEK293 cells expressing the human dopamine $D_{4.4}$ receptor. *Br. J. Pharmacol.* **1998**, *124*, 889–896.

(7) Gazi, L.; Sommer, B.; Nozulak, J.; Schoeffter, P. NGD 94-1 as an agonist at human recombinant dopamine $D_{4.4}$ receptors expressed in HEK293 cells. *Eur. J. Pharmacol.* **1999**, *372*, R9–R10.

(8) Lober, S.; Hubner, H.; Utz, W.; Gmeiner, P. Rationally based efficacy tuning of selective dopamine D4 receptor ligands leading to the complete antagonist 2-[4-(4-chlorophenyl)piperazin-1-ylmethyl]pyrazolo[1,5-*a*]pyridine (FAUC 213). *J. Med. Chem.* **2001**, *44*, 2691–2694.

(9) Boeckler, F.; Russig, H.; Zhang, W.; Löber, S.; Schetz, J.; Hübner, H.; Ferger, B.; Gmeiner, P.; Feldon, J. FAUC 213, a highly selective dopamine D_4 receptor full antagonist, exhibits atypical antipsychotic properties in behavioural and neurochemical models of schizophrenia. *Psychopharmacology* **2004**, *175*, 7–17.

(10) Corrigan, M. H.; Gallen, C. C.; Bonura, M. L.; Merchant, K. M. Effectiveness of the selective D_4 antagonist sonepiprazole in schizophrenia: a placebo-controlled trial. Sonepiprazole study group. *Biol. Psychiatry* **2004**, *55*, 445–451.

(11) Ebstein, R. P.; Novick, O.; Umansky, R.; Priel, B.; Osher, Y.; Blaine, D.; Bennett, E. R.; Nemanov, L.; Katz, M.; Belmaker, R. H. Dopamine D_4 receptor (D_4DR) exon III polymorphism associated with the human personality trait of novelty seeking. *Nat. Genet.* **1996**, *12*, 78–80.

(12) Ebstein, R. P.; Benjamin, J.; Belmaker, R. H. Personality and polymorphisms of genes involved in aminergic neurotransmission. *Eur. J. Pharmacol.* **2000**, *410*, 205–214.

(13) Dulawa, S. C.; Grandy, D. K.; Low, M. J.; Paulus, M. P.; Geyer, M. A. Dopamine D_4 receptor-knock-out mice exhibit reduced exploration of novel stimuli. *J. Neurosci.* **1999**, *19*, 9550–9556.

(14) Powell, S. B.; Paulus, M. P.; Hartman, D. S.; Godel, T.; Geyer, M. A. RO-10-5824 is a selective dopamine D4 receptor agonist that increases novel object exploration in C57 mice. *Neuropharmacology* **2003**, *44*, 473–481.

(15) Faraone, S. V.; Doyle, A. E.; Mick, E.; Biederman, J. Meta-analysis of the association between the 7-repeat allele of the dopamine D_4 receptor gene and attention deficit hyperactivity disorder. *Am. J. Psychiatry* **2001**, *158*, 1052–1057.

(16) Grady, D. L.; Chi, H. C.; Ding, Y. C.; Smith, M.; Wang, E.; Schuck, S.; Flodman, P.; Spence, M. A.; Swanson, J. M.; Moyzis, R. K. High prevalence of rare dopamine receptor D_4 alleles in children diagnosed with attention-deficit hyperactivity disorder. *Mol. Psychiatry* **2003**, *8*, 536–545.

(17) LaHoste, G. J.; Swanson, J. M.; Wigal, S. B.; Glabe, C.; Wigal, T.; King, N.; Kennedy, J. L. Dopamine D_4 receptor gene polymorphism is associated with attention deficit hyperactivity disorder. *Mol. Psychiatry* **1996**, *1*, 121–124.

(18) Swanson, J. M.; Sunohara, G. A.; Kennedy, J. L.; Regino, R.; Fineberg, E.; Wigal, T.; Lerner, M.; Williams, L.; LaHoste, G. J.; Wigal, S. Association of the dopamine receptor D_4 (DRD_4) gene with a refined phenotype of attention deficit hyperactivity disorder (ADHD): a family-based approach. *Mol. Psychiatry* **1998**, *3*, 38–41.

(19) Johansson, S.; Halleland, H.; Halmøy, A.; Jacobsen, K. K.; Landaas, E. T.; Dramsdahl, M.; Fasmer, O. B.; Bergsholm, P.; Lundervold, A. J.; Gillberg, C.; Hugdahl, K.; Knappskog, P. M.; Haavik, J. Genetic analyses of dopamine related genes in adult ADHD patients suggest an association with the DRD5-microsatellite repeat, but not with DRD_4 or SLC6A3 VNTRs. *Am. J. Med. Genet., Part B* **2008**, *147*, 1470–1475.

(20) Shaw, P.; Gornick, M.; Lerch, J.; Addington, A.; Seal, J.; Greenstein, D.; Sharp, W.; Evans, A.; Giedd, J. N.; Castellanos, F. X.; Rapoport, J. L. Polymorphisms of the dopamine D4 receptor, clinical outcome, and cortical structure in attention-deficit/hyperactivity disorder. *Arch. Gen. Psychiatry* **2007**, *64*, 921–931.

(21) Schetz, J. A.; Sibley, D. R. Dopaminergic Neurotransmission. In *Handbook of Contemporary Neuropharmacology*; Sibley, D., Hanin, I., Kuhar, M., Skolnick, P., Eds.; John Wiley & Sons, Inc.: Hoboken, NJ, 2007; pp 221−256.

(22) Zhang, K.; Tarazi, F. I.; Baldessarini, R. J. Role of dopamine D_4 receptors in motor hyperactivity induced by neonatal 6-hydroxydopamine lesions in rats. *Neuropsychopharmacology* **2001**, *25*, 624–632.

(23) Zhang, K.; Davids, E.; Tarazi, F. I.; Baldessarini, R. J. Serotonin transporter binding increases in caudate-putamen and nucleus accumbens after neonatal 6-hydroxydopamine lesions in rats: implications for motor hyperactivity. *Dev. Brain Res.* **2002**, *30*, 135–138.

(24) Browman, K. E.; Curzon, P.; Pan, J. B.; Molesky, A. L.; Komater, V. A.; Decker, M. W.; Brioni, J. D.; Moreland, R. B.; Fox, G. B. A-412997, a selective dopamine D_4 agonist, improves cognitive performance in rats. *Pharmacol., Biochem. Behav.* **2005**, *82*, 148–155.

(25) Brioni, J. D.; Moreland, R. B.; Cowart, M.; Hsieh, G. C.; Stewart, A. O.; Hedlund, P.; Donnelly- Roberts, D. L.; Nakane, M.; Lynch, J. J., III; Kolasa, T.; Polakowski, J. S.; Osinski, M. A.; Marsh, K.; Andersson, K.-E.; Sullivan, J. P. Activation of dopamine D_4 receptors by ABT-724 induces penile erection in rats. *Proc. Natl. Acad. Sci. U.S.A.* **2004**, *101*, 6758–6763.

(26) Collins, G. T.; Truccone, A.; Haji-Abdi, F.; Newman, A. H.; Grundt, P.; Rice, K. C.; Husbands, S. M.; Greedy, B. M.; Enguehard-Gueiffier, C.; Gueiffier, A.; Chen, J.; Wang, S.; Katz, J. L.; Grandy, D. K.; Sunahara, R. K.; Woods, J. H. Proerectile effects of dopamine D_2-like agonists are mediated by the D_3 receptor in rats and mice. *J. Pharmacol. Exp. Ther.* **2009**, *329*, 210–217.

(27) Patel, S.; Chapman, K. L.; Marston, D.; Hutson, P. H.; Ragan, C. I. Pharmacological and functional characterisation of dopamine D_4 receptors in the rat retina. *Neuropharmacology* **2003**, *44*, 1038–1046.

(28) Cohen, A. I.; Todd, R. D.; Harmon, S.; O'Malley, K. L. Photoreceptors of the mouse retina possess D_4 receptors coupled to adenylyl cyclase. *Proc. Natl. Acad. Sci. U.S.A.* **1992**, *89*, 12093–12097.

(29) Nir, I.; Harrison, J. M.; Haque, R.; Low, M. J.; Grandy, D. K.; Rubinstein, M.; Iuvone, P. M. Dysfunctional light-evoked regulation of cAMP in photoreceptors and abnormal retinal adaptation in mice lacking dopamine D_4 receptors. *J. Neurosci.* **2002**, *22*, 2063–2073.

(30) Matarrese, M.; Soloviev, D.; Moresco, R. M.; Todde, S.; Simonelli, P.; Colombo, D.; Magni, F.; Carpinelli, A.; Fazio, F.; Galli Kienle, M. Synthesis and in vivo evaluation of 3-[^{11}C]methyl-(3-methoxynaphthalen)-2-yl-(1-benzyl-piperidin)-4-yl-acetate (SB-235753), as a putative dopamine D_4 receptors antagonist for PET. *J. Labelled Compd. Radiopharm.* **2000**, *43*, 359–374.

(31) Eskola, O.; Bergman, J.; Lehikoinen, P.; Haaparanta, M.; Grönroos, T.; Forsback, S.; Solin, O. Synthesis of 3-[[4-(4-[^{18}F]fluorophenyl)-piperazin-1-yl]methyl]-1*H*-pyrrolo[2,3-*b*]pyridine. *J. Labelled Compd. Radiopharm.* **2002**, *45*, 687–696.

(32) Langer, O.; Halldin, C.; Chou, Y.; Sandell, J.; Swahn, C.; Någren, K.; Perrone, R.; Berardi, F.; Leopoldo, M.; Farde, L. Carbon-11 PB-12: an attempt to visualize the dopamine D_4 receptor in the primate brain with positron emission tomography. *Nucl. Med. Biol.* **2000**, *27*, 707–714.

(33) Zhang, M. R.; Haradahira, T.; Maeda, J.; Okauchi, T.; Kawabe, K.; Noguchi, J.; Kida, T.; Suzuki, K.; Suhara, T. Syntheses and pharmacological evaluation of two potent antagonists for dopamine D_4 receptors: [^{11}C]YM-50001 and *N*-[2-[4-(4-chlorophenyl)-piperizin-1-yl]ethyl]-3-[^{11}C]methoxybenzamide. *Nucl. Med. Biol.* **2002**, *29*, 233–241.

(34) Zhang, M. R.; Haradahira, T.; Maeda, J.; Okauchi, T.; Kawabe, K.; Kida, T.; Obayashi, S.; Suzuki, K.; Suhara, T. Synthesis and evaluation of 3-(4-chlorobenzyl)-8-[^{11}C]methoxy-1,2,3,4-tetrahydrochromeno[3,4-*c*]pyridin-5-one: a PET tracer for imaging $sigma_1$ receptors. *Nucl. Med. Biol.* **2002**, *29*, 469–476.

(35) Oh, S. J.; Lee, K. C.; Lee, S. Y.; Ryu, E. K.; Saji, H.; Choe, Y. S.; Chi, D. Y.; Kim, S. E.; Lee, J.; Kim, B. T. Synthesis and evaluation of fluorine-substituted 1*H*-pyrrolo[2,3-*b*]pyridine derivatives for dopamine D_4 receptor imaging. *Bioorg. Med. Chem.* **2004**, *12*, 5505–5513.

(36) Prante, O.; Tietze, R.; Hocke, C.; Löber, S.; Hübner, H.; Kuwert, T.; Gmeiner, P. Synthesis, radiofluorination, and in vitro evaluation of pyrazolo[1,5-*a*]pyridine-based dopamine D_4 receptor ligands: discovery of an inverse agonist radioligand for PET. *J. Med. Chem.* **2008**, *51*, 1800–1810.

(37) *ClogP*, version 4.0 (for Windows); BioByte Corp.: Claremont, CA.

(38) Pike, V. W. PET radiotracers: crossing the blood−brain barrier and surviving metabolism. *Trends Pharmacol. Sci.* **2009**, *30*, 431–340.

(39) Laruelle, M.; Slifstein, M.; Huang, Y. Relationships between radiotracer properties and image quality in molecular imaging of the brain with positron emission tomography. *Mol. Imaging Biol.* **2003**, *5*, 363–375.

(40) Waterhouse, R. N. Determination of lipophilicity and its use as a predictor of blood−brain barrier penetration of molecular imaging agents. *Mol. Imaging Biol.* **2003**, *5*, 376–389.

(41) Perrone, R.; Berardi, F.; Colabufo, N. A.; Leopoldo, M.; Tortorella, V. 1-(2-Methoxyphenyl)-4-alkylpiperazines: effect of the N-4 substituent on the affinity and selectivity for dopamine D_4 receptor. *Bioorg. Med. Chem. Lett.* **1997**, *7*, 1327–1330.

(42) Perrone, R.; Berardi, F.; Colabufo, N. A.; Leopoldo, M.; Tortorella, V. *N*-[2-[4-(4-Chlorophenyl)piperazin-1-yl]ethyl]-3-methoxybenzamide: a potent and selective dopamine D_4 ligand. *J. Med. Chem.* **1998**, *41*, 4903–4909.

(43) Perrone, R.; Berardi, F.; Colabufo, N. A.; Leopoldo, M.; Tortorella, V. A structure−affinity relationship study on derivatives of *N*-[2-[4-(4-chlorophenyl)piperazin-1-yl]ethyl]-3-methoxybenzamide, a high-affinity and selective D_4 receptor ligand. *J. Med. Chem.* **2000**, *43*, 270–277.

(44) Jung, H. K.; Doddareddy, M. R.; Cha, J. H.; Rhim, H.; Cho, Y. S.; Koh, H. Y.; Jung, B. Y.; Pae, A. N. Synthesis and biological evaluation of novel T-type Ca^{2+} channel blockers. *Bioorg. Med. Chem.* **2004**, *12*, 3965–3970.

(45) Ishizumi, K.; Kojima, A.; Antoku, F. Synthesis and anxiolytic activity of N-substituted cyclic imides (1*R**,2*S**,3*R**,4*S**)-*N*-[4-[4(2-pyrimidinyl)-1-piperazinyl]butyl]-2,3-bicyclo[2.2.1]heptanedicarboximide (tandospirone) and related compounds. *Chem. Pharm. Bull.* **1991**, *39*, 2288–2300.

(46) Leopoldo, M.; Berardi, F.; Colabufo, N. A.; De Giorgio, P.; Lacivita, E.; Perrone, R.; Tortorella, V. Structure−affinity relationship study on *N*-[4-(4-arylpiperazin-1-yl)butyl]arylcarboxamides as potent and selective dopamine D_3 receptor ligands. *J. Med. Chem.* **2002**, *45*, 5727–5735.

(47) Enguehard-Gueiffier, C.; Gueiffier, A. Recent progress in medicinal chemistry of D_4 agonists. *Curr. Med. Chem.* **2006**, *13*, 2981–2993.

(48) Lee, I. T.; Chen, S.; Schetz, J. A. An unambiguous assay for the cloned human sigma$_1$ receptor reveals high affinity interactions with dopamine D_4 receptor selective compounds and a distinct structure−affinity relationship for butyrophenones. *Eur. J. Pharmacol.* **2008**, *578*, 123–136.
(49) Halldin, C.; Gulyás, B.; Langer, O.; Farde, L. Brain radioligands—state of the art and new trends. *Q. J. Nucl. Med.* **2001**, *45*, 139–152.
(50) Primus, R.; Thurkauf, A.; Xu, J.; Yevich, E..; Mcinerney, S.; Shaw, K.; Tallman, J. F.; Gallager, D. W. Localization and characterization of dopamine D_4 binding sites in rat and human brain by use of the novel, D_4 receptor-selective ligand [^{3}H]NGD 94-1. *J. Pharmacol. Exp. Ther.* **1997**, *282*, 1020–1027.
(51) De La Garza, R.; Madras, B. K. [^{3}H]PNU-101958, a D_4 dopamine receptor probe, accumulates in prefrontal cortex and hippocampus of non-human primate brain. *Synapse* **2000**, *37*, 232–244.
(52) Marazziti, D.; Baroni, S.; Masala, I.; Giannaccini, G.; Betti, L.; Palego, L.; Catena Dell'Osso, M.; Consoli, G.; Castagna, M.; Lucacchini, A. [^{3}H]-YM-09151-2 binding sites in human brain postmortem. *Neurochem. Int.* **2009**, *55*, 643–647.
(53) Inoue, O.; Kobayashi, K.; Gee, A. Changes in apparent rates of receptor binding in the intact brain in relation to the heterogeneity of reaction environments. *Crit. Rev. Neurobiol.* **1999**, *13*, 199–225.
(54) Caccia, S. N-Dealkylation of arylpiperazine derivatives: disposition and metabolism of the 1-aryl-piperazines formed. *Curr. Drug Metab.* **2007**, *8*, 612–622.
(55) Steuer, H.; Jaworski, A.; Stoll, D.; Schlosshauer, B. In vitro model of the outer blood−retina barrier. *Brain Res. Protoc.* **2004**, *13*, 26–36.
(56) Kyle, D. J.; Sun, Q. Preparation of Piperazine Compounds as VR1 Inhibitors. PCT Int. Appl. WO 2005012287, 2005; *Chem. Abstr.* **2005**, *142*, No. 198104.
(57) Leopoldo, M.; Lacivita, E.; De Giorgio, P.; Colabufo, N. A.; Niso, M.; Berardi, F.; Perrone, R. Design, synthesis, and binding affinities of potential positron emission tomography (PET) ligands for visualization of brain dopamine D_3 receptors. *J. Med. Chem.* **2006**, *49*, 358–365 and references cited therein .
(58) Avdeef, A.; Box, K. J.; Comer, J. E.; Gilges, M.; Hadley, M.; Hibbert, C.; Patterson, W.; Tam, K. Y. pH-metric logP11. pK_a detrmination of water-insoluble drugs in organic solvent−water mixtures. *J. Pharm. Biomed. Anal.* **1999**, *20*, 631–641.
(59) Noguchi, J.; Suzuki, K. Automated synthesis of the ultra high specific activity of [^{11}C]Ro15-4513 and its application in an extremely low concentration region to an ARG study. *Nucl. Med. Biol.* **2003**, *30*, 335–343.
(60) Ericksen, S. S.; Cummings, D. F.; Weinstein, H.; Schetz, J. A. Ligand selectivity of D_2 dopamine receptors is modulated by changes in local dynamics produced by sodium binding. *J. Pharmacol. Exp. Ther.* **2009**, *328*, 40–54.
(61) Cummings, D. F.; Ericksen, S. S.; Schetz, J. A. Three amino acids in the D_2 dopamine receptor regulate selective ligand function and affinity. *J. Neurochem.* **2009**, *110*, 45–57.
(62) Cummings, D. F.; Canseco, D. C..; Sheth, P.; Johnson, J. E.; Schetz, J. A. Synthesis and structure−affinity relationships of novel small molecule natural product derivatives capable of discriminating between serotonin 5-HT_{1A}, 5-HT_{2A}, 5-HT_{2C} receptor subtypes. *Bioorg. Med. Chem.* **2010**, *18*, 4783–4792.
(63) Kortagere, S.; Gmeiner, P.; Weinstein, H.; Schetz, J. A. Certain 1,4-disubstituted aromatic piperidines and piperazines with extreme selectivity for the dopamine D_4 receptor interact with a common receptor microdomain. *Mol. Pharmacol.* **2004**, *66*, 1491–1499.
(64) Cheng, Y. C.; Prusoff, W. H. Relationship between the inhibition constant (K_i) and the concentration of inhibitor which causes 50 per cent inhibition (IC_{50}) of an enzymatic reaction. *Biochem. Pharmacol.* **1973**, *22*, 3099–3108.
(65) Watanabe, M.; Okada, H.; Shimizu, K.; Omura, T.; Yoshikawa, E.; Kosugi, T.; Mori, S.; Yamashita, T. A high resolution animal PET scanner using compact PS-PMT detectors. *IEEE Trans. Nucl. Sci.* **1997**, *44*, 1277–1282.
(66) Maeda, J.; Suhara, T.; Kawabe, K.; Okauchi, T.; Obayashi, S.; Hojo, J.; Suzuki, K. Visualization of α5 subunit of $GABA_A$/benzodiazepine receptor by [^{11}C]Ro15-4513 using positron emission tomography. *Synapse* **2003**, *47*, 200–208.